Characterization of the Atlantic Water and Levantine Intermediate Water in the Mediterranean Sea using 20 years of Argo Data

Fedele Giusy[1,*], Mauri Elena [1], Notarstefano Giulio [1] and Poulain Pierre Marie[1]

(1) National Institute of Oceanography and Applied Geophysics, OGS, 34010 Sgonico (TS), Italy

* Corresponding author (gfedele@inogs.it)

The Atlantic Water (AW) and Levantine Intermediate Water (LIW) are important water masses that play a crucial role in the internal variability of the Mediterranean thermohaline circulation. In particular, their variability and interaction, along with other water masses that characterize the Mediterranean basin, such as the Western Mediterranean Deep Water (WMDW), contribute to modify the Mediterranean Outflow through the Gibraltar Strait and hence may influence the stability of the global thermohaline circulation.

This work aims to characterize the AW and LIW in the Mediterranean Sea, taking advantage of the large observational dataset provided by Argo floats from 2001 to 2019. Using different diagnostics, the AW and LIW were identified, highlighting the inter-basin variability and the strong zonal gradient that denote the two water masses in this marginal sea. Their temporal variability was also investigated in the last two-decades, providing a more robust view of the AW and LIW characteristics, which in previous studies, due to lack of data, have been investigated taking advantage of very short periods.

A clear salinification and warming trend characterize the AW and LIW in the last two decades (~0.007$\pm$0.140 and 0.006 $\pm$0.038 yr^{-1}; 0.026$\pm$0.715 and 0.022$\pm$0.232 °C yr^{-1}, respectively). The salinity and temperature trends found at subbasin scale are in good agreement with previous results. The strongest trends are found in the Adriatic basin in both the AW and LIW properties.

Keywords: Argo, Atlantic Water, Interannual variability, Inter-basin variability, Levantine Intermediate Water, Mediterranean Sea, Trends

Acknowledgments

This research was funded by the Italian Ministry of University and Research as part of the Argo-Italy program.

1 Introduction

The Atlantic Water (AW) and Levantine Intermediate Water (LIW) play a central role in the internal variability of the Mediterranean thermohaline circulation, contributing to the dense water formation in this enclosed basin (Tsimplis et al., 2006). The variability and interaction of these two water masses modulate the Mediterranean outflow through the Gibraltar Strait, which plays an important role on the North Atlantic oceanic variability, and in turn to the stability of the global thermohaline circulation (e.g., Rahmstorf, 2006; Hernandez-Molina et al., 2014). Therefore, from a climatic point of view, it is relevant to characterize their main properties and monitor their variability, which are the main purpose of this paper.

Flowing in the Mediterranean Sea through the Gibraltar strait, the AW is less dense than the surrounding water masses and therefore it populates most of the Mediterranean surface layer. Its path is mainly driven by the Coriolis effect and by the complex topography that characterizes this region (Millot and Taupier-Letage 2005).

The LIW is the most voluminous water mass produced in the Mediterranean Sea (e.g., Skliris 2014; Lascaratos et al., 1993), and the saltiest water formed with a relatively high temperature at intermediate depths. It is formed in the Levantine subbasin, after which it is named, where one of the main formation sites is the Rhodes Gyre (e.g., Tsimplis et al., 2006; Kubin et al., 2019). The LIW strongly influences the thermohaline circulation, flowing at intermediate depths and then passing over the sills, exiting the Gibraltar Strait and modifying the Atlantic circulation (Rahmstorf, 1998; Bethoux et al., 1999).

Several studies have been devoted to the analysis of the AW and LIW main features and variability, taking advantage of different indicators to identify and track these two water masses in the Mediterranean Sea. Among them, the AW and the LIW are usually referred to the minimum and maximum salinity in the surface and intermediate layers of the water column, respectively (e.g., Millot and Taupier-Letage 2005; Bergamasco and Malanotte-Rizzoli, 2010; Mauri et al., 2019; Juza et al., 2019; Kokkini et al., 2019; Várgas-Yañez et al., 2020). However, different approaches can also be found in the literature. In particular Millot (2014) associated the LIW to the maximum of the potential temperature vertical gradient found in an intermediate water layer, while Bosse et al. (2015) identified the LIW in the northwestern Mediterranean Sea with the maximum salinity value found between two potential density values ($\sigma_\theta = [29.03 - 29.10]\frac{kg}{m^3}$), encompassing both temperature and salinity maxima characterizing the LIW layer. The main findings related to the hydrological properties of these two water masses are summarized below.

The AW enters in the Mediterranean Sea through the Gibraltar Strait, occupying the upper 200 m of depth with potential density, temperature and salinity annual mean values: $\sigma_\theta \cong [26.5 - 27]\frac{kg}{m^3}, T \cong [14 - 16]°C, S \cong [36.0 - 36.5]$ respectively (e.g., Bergamasco and Malanotte-Rizzoli, 2010; Hayes et al., 2019). The AW flowing at the surface, continuously interacts with the atmosphere and is subject to evaporation and mixing with the underlying water masses. Flowing eastward, it becomes denser and the minimum salinity core sinks. Therefore, it can be capped by the surface mixed layer and less influenced by air-sea interactions. Its properties and variability are also modified by the local eddies and by the river discharges in the coastal regions. These mechanisms shape the AW, leading to an increase of salinity from about 36.25 in the Gibraltar Strait to values around 39.2 in the Levantine Sea (e.g., Bergamasco and Malanotte-Rizzoli, 2010; Hayes et al., 2019). These values highlight strong AW temperature and salinity gradients between the Western Mediterranean (WMED) and the Eastern Mediterranean (EMED).

The properties of the LIW core in the WMED are commonly referred to the following ranges of potential density, temperature, salinity and depth, respectively: $\sigma_\theta = [29 - 29.10]\frac{kg}{m^3}, T = [13 - 14.2]°C, S = [38.4 - 38.8], D = [200 - 600]m$ (e.g. Millot, 2013; Hayes et al., 2019;

Várgas-Yañez et al., 2020); while in the EMED these properties span over different values: $\sigma_\theta = [28.85 - 29.15]\frac{kg}{m^3}, T = [14.6 - 16.4]°C, S = [38.85 - 39.15], D = [150 - 400]m$ (e.g. Lascaratos et al., 1993; Hayes et al., 2019). Therefore, moving westward, *T* and *S* decrease and the LIW sinks.

These studies provide a general view of the AW and LIW properties in the Mediterranean Sea, highlighting a strong inter-basin variability of these water masses along their paths, which in turn influences their temporal changes.

An example is given by a recent paper by Kassis and Korres (2020), which provides a detailed view of the EMED hydrographic properties for the period 2004–2017 taking advantage of Argo data. Exploring the water column from the surface down to 1500 m in seven different regions of the EMED, they revealed a high inter-annual variability of the stored heat and salt over this region.

In this study, following a similar approach, we investigate the AW and LIW properties, isolating their main characteristics and variability from the surrounding water masses, taking advantage of several diagnostics discussed in section 2.2. Our work aims to provide a more robust view of the AW and LIW characteristics, which in previous studies, due to lack of data, have been investigated taking advantage of short periods.

In the frame of climate change studies, it is important to estimate possible impacts of AW and LIW changes on the Mediterranean climate, since this region is one of the most vulnerable climate change hotspots (Giorgi 2006). In fact, changes in temperature and salinity can strongly affect the marine system over the Mediterranean and related human activities.

Previous studies highlighted a clear salinification of the Mediterranean Sea over the past few decades (e.g., Painter and Tsimplis 2003; Vargas -Yáñez et al., 2010; Schroeder et al., 2017; Skliris et al., 2018) and a clear deep water warming trend after 1980s, which in literature is often related to the Nile River damming and to the global warming (Vargas-Yáñez et al., 2010). Positive temperature and salinity trends, oscillating between [0.0016÷0.0091] °C/yr and [0.0008÷0.001] yr^{-1}, respectively, are found in the deep layer (below ~700 meters) between 1950 to 2005 (e.g., Bethoux et al., 1990; Rohling and Bryden, 1992; Millot et al., 2006; Vargas-Yáñez et al., 2010; Borghini et al., 2014).

106 This observed salinification and warming are also found at intermediate depths in several
107 studies (e.g., Zu et al., 2014; Schroeder et al., 2017; Skliris et al., 2018), with ranges that depend
108 on the region of investigation. A clear positive salinity trend between 150-600 m is found in the
109 Mediterranean Sea by Skliris et al. (2018), analyzing the MEDATLAS data from 1950 to 2002
110 (~0.007±0.004 yr^{-1}).
111 In contrast, heterogeneous temperature trends are found in the upper layer in different regions
112 (Painter and Tsimplis, 2003). This sensitivity of the trends to the area of interest, can be due to
113 several reasons, such as the changes in the large-scale atmospheric forcing of the Mediterranean
114 region, the river runoff which differ from one region to another, and to the data coverage over a
115 specific area (e.g., Painter and Tsimplis, 2003; Vargas -Yáñez et al., 2009; 2010). In this respect,
116 Vargas -Yáñez et al. (2009) highlighted that the scarcity of data makes trend estimations very
117 sensitive to the data postprocessing, comparing results from different studies dealing with the
118 same time period. Therefore, in order to reduce the uncertainty of the trend estimations, longer
119 and less sparse timeseries are needed.
120 In this respect, this work aims to provide an updated view of the temporal evolution and trends
121 of the AW and LIW, taking advantage of the large observational dataset provided by the MedArgo
122 Program (Poulain et al., 2007). It covers the water column from the surface down to ~2000 m
123 over the entire Mediterranean basin from 2001 to 2019. The Mediterranean Sea has been widely
124 studied through the deployment of hundreds of Argo profiling floats (Argo 2020) in the last two
125 decades as part of various national, European and international programs (Wong et al., 2021) and
126 with the participation of different institutions. For these reasons, this dataset constitutes an optimal
127 observational framework to investigate the AW and LIW properties.
128 The dataset and the methods used in this study are described in section 2, the results are
129 presented in section 3, where the inter-basin and inter-annual variabilities of the AW and LIW in
130 the Mediterranean Sea are shown. The main conclusions are drawn in section 4.
131

132 ## 2 Data and method

133 ### 2.1 Data

In this work the AW and LIW properties in the Mediterranean Sea are investigated taking advantage of the Argo float dataset, which consists of more than thirty thousand *T-S* profiles for the period 2001–2019. Since 2001, the number of observations is generally increasing, reaching a peak of 4188 profiles in 2015, mainly thanks to the combined efforts of national and international Argo initiatives. The deployments of most Argo floats in the Mediterranean were coordinated by the MedArgo regional center (Poulain et al., 2007). In the Mediterranean, the cycling period is usually reduced to 5 days, and the maximum profiling depth is mostly 700 or 2000 m (Poulain et al., 2007). The floats are equipped with Sea-Bird Conductivity-Temperature-Depth (CTD) sensors (model SBE41CP; www.seabird.com/sbe-41-argo-ctd/product-details?id=54627907875) with accuracies of ±0.002° C, ±0.002 and ±2 dbar for temperature, salinity and pressure, respectively. The data measured by the profilers are transmitted to satellites (e.g., via the Iridium or Argos telemetry systems), then to ground receiving stations, processed and real-time quality-controlled by the Argo Data Assembly Centres (https://www.euro-argo.eu/Activities/Data-Management/Euro-Argo-Data-Centres), sent to the Global Data Assembly Center and made available for free to users (https://fleetmonitoring.euro-argo.eu/dashboard?Status=Active). The delayed-mode quality control applied on pressure, temperature and salinity follows the guidelines described in the Argo Quality Control Manual for CTD (e.g., Wong et al., 2021; Cabanes et al., 2016), in conjunction with other procedures developed at regional level (Notarstefano and Poulain, 2008; Notarstefano and Poulain, 2013) to check the salinity data and any potential drift of the conductivity sensor.

The analyses are performed in eight Mediterranean sub-basins following the climatological areas defined by the EU/MEDARMEDATLAS II project (http://nettuno.ogs.trieste.it/medar/climatologies/medz.html), emphasizing the processes that take place in each sub-basin and modify the water mass properties. Fig. 1 shows the geographical distribution of the Argo profiles from 2001 to 2019 in the eight sub-basins considered (Algerian, Catalan, Ligurian, Tyrrhenian, Adriatic, Ionian, Cretan and Levantine). The Alboran, Aegean and the Sicily Channel sub-basins are not analyzed in this work due to the scarcity of observations in these areas.

Most sub-basins are well spatially covered, except for the Adriatic Sea, where the majority of observations are concentrated in the South Adriatic Pit (SAP) and therefore it is important to keep in mind that the results found for this region, are representative of the southern Adriatic Sea. The SAP is an important deep water convection site in the Mediterranean Sea (e.g., Kokkini et al., 2019; Mauri et al., 2021; Mihanović et al. (2021); Azzaro et al., 2012; Bensi et al., 2013) and therefore it is also considered as a crucial area from a climatic perspective. The temporal distribution of the float data is different in the various sub-basins: the longest time series are available in the Ionian, Cretan and Levantine regions, with data from 2001 to 2019, followed by the Algerian, Ligurian and Tyrrhenian sub-basins where data are available after 2003, and then by the Adriatic Sea with data only after 2009. In this context, it is important to mention that the low density in space and time of the Argo profiles induces uncertainties in the results, especially during the first years of the analyzed period.

2.2 Methods

As discussed in the introduction, many indicators/characteristics have been adopted in literature to track the AW and LIW in the Mediterranean Sea. Most of them consider, as best indicator, the minimum/maximum salinity at surface/intermediate layer for the AW/LIW and motivated us to follow a similar approach (e.g., Millot and Taupier-Letage, 2005; Bergamasco and Malanotte-Rizzoli, 2010; Hayes et al., 2019; Lamer et al., 2019).

A preliminary step in this analysis was the post-processing: we first applied a time sub-sampling on each profiler to obtain a more homogeneous dataset (Notarstefano and Poulain, 2009). This is applied to each float as follows: if the cycling period is 1 day or less, the profiles are sub-sampled every 5 days; if the period is 2 or 3 days, they are sub-sampled every 6 days; and if the period is 5 or 10 days, no subsampling is applied. Afterward, each profile was linearly interpolated from the surface (0 m) to the bottom every 10 m to obtain comparable profiles; and finally, a running filter with a 20 m window, was applied to the data along the depth axis, to smooth any residual spike.

189 Finally, the minimum/maximum salinity value in each profile is associated to the AW/LIW
190 core in the respective depth layer. Then, the correspondent depth and temperature values are
191 considered.
192 Once the AW and LIW core are identified in each profile, the AW and LIW inter-basin
193 variabilities were analyzed taking advantage of the boxplot approach applied to each parameter
194 and region (Fig. 2). In Fig.2, the whiskers (black dashed line out of the box) extend to the most
195 extreme data points not considering the outliers at the 5% significance level ($pvalue \leq 0.05$). In
196 order to test the significance, the Student's t distribution was applied to each hydrological
197 parameter in every sub-basin (Kreyszig and Erwin 1970). The null hypothesis (that states that the
198 population is normally distributed) is rejected with a 5% level of statistical significance. This
199 method is also applied to the timeseries trends. In section 3.1 we often refer to the range and
200 skewness of the distributions, that are the difference between the upper and lower limits and the
201 measure of the symmetry of the distributions, respectively (including only the 5% significance
202 values).
203 Considering only the AW/LIW salinity, temperature, and depth values at 95% level of
204 significance (Fig.2), as done for the spatial analysis, the timeseries from 2001 to 2019 have been
205 computed in each subbasin to analyze the low frequency variability (LFV) and trends at
206 interannual to decadal timescale over the available observed periods. In this respect, the high
207 frequency variability was filtered out, first by subtracting the mean seasonal cycle to the raw
208 timeseries, and then applying a median yearly average filter. This last step is needed since the
209 data are not homogeneous in time in every subbasin from 2001 to 2019, and therefore without it,
210 the seasonal variability can contaminate the estimation of the trends. The latter have been
211 computed using the linear least-squares method to fit a linear regression model to the data.
212

213 ## 3 Results and discussion

214 In this section, the AW and LIW properties are investigated in the eight Mediterranean climatic
215 regions before mentioned, focusing both on their spatial and temporal variability. The analysis of
216 the trends and spectral features are also shown.

3.1 Inter-basin variability

(i) AW

The hydrological properties of the AW core in eight sub-basins (Fig. 1) are shown in Figs. 2a, b, c, providing a compact view of the AW inter-basin variability for each parameter using the boxplot approach.

Moving eastward, the AW salinity increases from ~36 to 39.5 (minimum and maximum whiskers limits; Fig. 2a), since the surface salinity minimum is progressively smoothed by horizontal mixing with surrounding saltier waters. In fact, as discussed by Font et al. (1998) the AW minimum salinity is dependent on the different degrees of mixing due to its residence times.

In the Algerian sub-basin, the salinity range reaches the highest extension compared to the other regions, probably due to the large baroclinic instability that produces high mesoscale variability in the surface layer and horizontal mixing by strong eddies (Demirov and Pinardi 2007).

The AW salinity range is smaller in the Catalan, Ligurian and Tyrrhenian Seas, where similar distributions are found both in terms of range and skewness (which is close to zero): the main mode and the median have salinity of ~38. In the Adriatic Sea the distribution is probably skewed toward higher values because a clear positive salinity trend is found (Fig. 3; Lipizer et al., 2014). In the Adriatic, Ionian and Cretan Seas, the range is higher than the surrounding sub-basins: in the Adriatic and Ionian Sea this could be associated to the Bimodal Oscillation System (BiOS), and then to the reversal of the North Ionian Gyre (Rubino et al., 2020), while in the Cretan Sea we speculate that it is caused by the sinking of the AW during winter. This is in agreement with Schroeder (2019), where it is shown that in the Cretan Sea, the strong wind-induced evaporation and heat loss during winter lead the AW transformation into salty and warm Cretan Intermediate Water. The depths reached in the Cretan basin (Fig. 2c) seem to confirm this hypothesis.

The AW temperature is highly variable, ranging between ~5 and ~30 °C, with a wider range in the Catalan and Adriatic regions (Fig. 2b), possibly due to the higher seasonal sea surface temperature variability over these sub-basins (Shaltout and Omstedt 2014). The lowest

245 temperatures detected can be related to the freshwater fluxes in these regions. In this respect, an
246 episode that can be relevant for the AW distribution in the Adriatic Sea is the large river runoff
247 observed in 2014 by Kokkini et al. (2019), which caused a saline stratification for more than a
248 year. This episode is also captured by our analyses (Fig. 3). As observed for the AW salinity
249 mode, even the temperature mode shift toward higher values moving eastward in agreement with
250 the literature (Bergamasco and Malanotte-Rizzoli 2010). In the Algerian basin the AW
251 temperature mode is higher than it is in the Catalan subbasin: this can be due to the influence of
252 freshwater fluxes in the Catalan region and led by the high eddy activity over the Algerian region
253 (Escudier et al., 2016) led by the strong baroclinic instability already discussed for the salinity
254 field (e.g., Demirov and Pinardi 2007; Cotroneo et al., 2016; Aulicino et al., 2018; Aulicino et al.,
255 2019). The temperature and salinity ranges captured in the Algerian region are in good agreement
256 with those found by Cotroneo et al. (2020) and shown in their Table 2.
257 The depths of the AW core oscillate between 0 and 90 m with the main mode sinking eastward
258 (Fig. 2c). The distributions are all skewed toward lower depths, with the maximum probability
259 density function (PDF) near surface and a median shifting from 0 to 45 m moving eastward,
260 indicating a clear sinking of the AW along its pathway.
261
262 (ii) LIW
263 In this section, the main hydrological properties of the LIW are analyzed in each sub-basin.
264 Flowing away from the region of formation, the LIW interacts with the surrounding water
265 masses and becomes less salty; the salinity sharply drops from ~39.2 to ~38.5, moving from the
266 Levantine to the Ligurian subbasin, and then it becomes more stable in the Algerian and Catalan
267 regions, oscillating around ~38.5 (Fig.2e). The distributions are highly symmetric around the
268 median and the variability decreases flowing westward maybe because the LIW becomes deeper,
269 sinking from ~100 to ~650 m (Fig. 2g). The highest salinity is reached in the Cretan basin, where
270 the formation of salty and warm Cretan Intermediate Water, caused by strong wind-induced
271 evaporation and heat loss during winter, influences the LIW properties and detection (Schroeder,
272 2019).

The LIW temperature decreases westward from ~18 to ~12.8 °C. The range is higher in the EMED as also found for salinity, suggesting that over this region, the intrusion of warmer and saltier surface waters due to convective processes characterizes the LIW formation (Fig. 2f; Schroeder, 2019).

The sinking of the LIW flowing westward is shown in Fig. 2g, dropping from about 100 to 650 m (maximum whiskers values). The distributions tend to be symmetric in most of the Mediterranean Sea, except for the Adriatic Sea, where a strong LIW bimodality in the depth domain is found, with two peaks located at ~190 and ~500 m respectively (here not shown), in agreement with Kokkini et al. (2019) and Mihanović et al. (2021). In this respect, Mihanović et al. (2021), analyzing observed data from CTD measurements, Argo floats, several glider missions, satellite observations and operational ocean numerical model products, provides a possible explanation to this double-maxima vertical pattern, suggesting that these two peaks may be explained by two concurrent events: the winter convection at the beginning of 2017, which leads higher salinities in the water column, and a very strong inflow of high salinity waters from the Northern Ionian in late winter and spring of 2017, which this time is restricted almost to the surface.

3.2 Interannual variability

In this section, the temporal variability of the AW and LIW in each sub-basin is studied analyzing the 1-year moving average timeseries and the relative trends.

The results of this analysis are affected by the irregular spatial and temporal sampling of the Argo floats. Time gaps in the data are found in the Catalan, Tyrrhenian and Cretan Seas (Fig. 3). The missing data are due to the lack of Argo float samplings. Data in the Adriatic Sea are available only after 2009, while the Ionian, Cretan and Levantine sub-basins have much longer timeseries, with data covering the period from 2001 to 2019.

3.2.1 Trends

(i) AW trends

The AW salinity temporal evolution is shown in Fig. 3, where significant trends (at 5% level of significance) are found in each region (Table 1). Positive trends are clearly found in the EMED and in the Tyrrhenian Sea, highlighting a clear salinification of the AW in the last two decades over most of the Mediterranean Sea (~0.007±0.140 yr^{-1}; Table 1). Comparable positive salinity trends between 0-150 m (~0.009±0.009 yr^{-1}) are also found in Skliris et al. (2018) where multi-decadal salinity changes in the Mediterranean Sea are investigated taking advantage of the MEDATLAS database (MEDAR Group 2002) consisting of temperature and salinity profiles in the Mediterranean from 1945 to 2002 (https://www.bodc.ac.uk/resources/inventories/edmed/report/4651/). A clear meridional separation is found in the AW trends during the observed period. In the Tyrrhenian Sea and in the entire EMED the AW becomes saltier, with significant positive trends, whilst in the WMED, a significant negative trend emerges in the Algerian and Catalan subbasins (Table 1). This freshening of the AW inflow could be related to the observed rapid freshening of the North Atlantic Ocean (Dickson et al. 2002), which causes are related to different phenomenon, included the accelerating Greenland melting triggered by the global warming (Dukhovskoy et al., 2019). These findings seem in contradiction with the results provided by Millot (2007), showing a salinification of the Mediterranean outflow, obtained analyzing autonomous CTDs on the Moroccan shelf in the strait of Gibraltar in the period 2003-2007, which may be caused by the different epochs under study. In fact, comparing Fig. 3 in Millot (2007) and Fig. 3 in this work, a similar positive trend is captured in the Algerian sub-basin, in the same period; while extending the analysis to a longer timeseries, a clear negative trend leads the AW variability at interannual to decadal timescale. Opposite trends are found in the EMED and in the Tyrrhenian subbasin, where the very strong increase in net evaporation of ~8 to 12% over 1950-2010 (Skiliris et al., 2018) and the damning of the Nile River (as projected by Nof, 1979) may have caused the AW salinification. The trends are steep in the Adriatic and Cretan sub-basins, where the salinity increases with an order of magnitude higher ($O[10^{-2}]$) and the largest increase is found in the Adriatic Sea (0.044±0.188 yr^{-1}). Here the impact of the negative E-P anomalies and large river runoff observed by Kokkini et al. (2019) around 2014 is well captured by the salinity time series.

329 The results in the EMED are in good agreement with Fig. 9 of Kassis and Korres (2020), where
330 the yearly average salinity per depth zone and per region between 2004-2017 are shown.
331 Similarities in the observed trend in the Ionian Sea ($0.009 \pm 0.181\ yr^{-1}$) are also found by Zu
332 et al., 2014 ($\text{mean trend} \sim 0.011\ yr^{-1}$), where the Argo floats data between 2004 and 2014 are
333 analyzed.

334 According to the above-mentioned meridional salinity transition from negative to positive
335 salinity trends moving eastward, the temperatures also show a meridional shift from positive to
336 negative significant trends east of the Ionian Sea, with a mean positive AW temperature trend
337 over the eight analyzed sub-basins (0.026 ± 0.715 °C/yr; Table 1). Interbasin changes between
338 the subbasins are instead linked to changes in the large-scale meteorological forcing of the
339 Mediterranean region (Painter and Tsimplis, 2003). As found for the salinity field, the sharper
340 increase is related to the Adriatic Sea ($\sim 0.117 \pm 0.951$ °C/year), highlighting the presence of
341 mechanisms that enhance the trends over this region. A sharpening in the trend over the last
342 decade is captured in the Catalan subbasin (Fig.7) and confirmed by Schuckmann et al. (2019),
343 who observed the same behavior in the Northwestern Mediterranean with a trend over the last
344 decade (~0.047 °C/yr), that doubles the respective trend in the previous 1982-2011 period (0.029
345 °C/yr).
346 The AW depths time series (Fig. 5) show a heterogeneous trend in the Mediterranean Sea,
347 with significant negative values (the depth decreases) in the Algerian and Ionian subbasins, and
348 positive in the Tyrrhenian and Levantine regions (Table 1), which reflects into a tendency of the
349 AW to become shallower, increasing the stratification at basin scale (0.238 ± 10.537 m/yr). Wider
350 temporal changes are found in the Levantine region, where the trend is from one to two orders of
351 magnitude higher than the other regions.
352

353 (ii) LIW

354 The LIW temporal variability is hereafter analyzed. Fig. 6 shows the salinity changes from
355 2001 to 2019 in the eight subbasins considered. A positive trend is found in the whole

Mediterranean Sea at 5% level of significance, highlighting a salinification also at intermediate depths of this enclosed basin over two decades (~0.006 $\pm$0.038 yr^{-1}; Table 1). A similar positive trend between 150-600 m is found by Skliris et al. (2018), in the MEDATLAS data from 1950 to 2002 (~0.007$\pm$0.004 yr^{-1}), with lower standard deviations. The higher standard deviations found in this study, compared to those founds by Skliris et al. (2018) could be related to the wider range of depths considered and to the different epochs considered. The LIW properties vary less than the AW in most of the basin, except for the Ligurian, and Levantine regions, where deep water and LIW water formations occur respectively. The strongest salinity increase is found in the Adriatic Sea (0.021$\pm$0.074 yr^{-1}), exceeding the trends in other regions by one order of magnitude. The Adriatic salinity trend from 2008 to 2018 is about five times larger than the Adriatic salinity trend observed in the period 1952-2010 and quantified by Vilibić et al. (2013). The possible source of such a large trend, may come by the biasing of the signal by the BiOS oscillations, since the series starts in 2008, when the anticyclonic BiOS was present. Here, the periodicity of the BiOS has a magnitude which is comparable with the timeseries length in the Adriatic, which might be also relevant for other sub-regions. Therefore, longest timeseries are needed to better estimate the trend over this sub-basin.

The LIW salinity positive trends over the Mediterranean Sea are also found by Zu et al. (2014), which confirms the salinification of the basin at intermediate depths, as also observed at surface in most of the analyzed regions. This suggests that the enhancement of the net evaporation over the Mediterranean in the last decades, that was observed by Skiliris et al. (2018), may lead the formation of saltier LIW in the EMED, and as consequence a mean positive salinity trend over the whole basin. While, in the WMED, positive trends (0.008$\pm$0.002; 0.009$\pm$0.0007 yr^{-1}; from gliders missions) are found from 2011 to 2017 by Juza et al. (2019), in agreement with the positive trends found in the last few years in the western subbasins shown in Fig.6.

Positive temperature trends (5% level of significance) are found in the whole Mediterranean Sea except in the Levantine sub-basin, where the negative trend could be related to oscillations with decadal timescales that take place over this region. This is confirmed by the continuous wavelet transforms applied to the timeseries (not shown). Peaks of salinity and temperature are

observed in ~2009 in the Levantine basin and then reach the Cretan Sea in ~2010. The same variability is discussed in Ozer et al. (2017) and explained in connection with the Ionian Bimodal Oscillating System (BiOS). These maxima are in fact attributed to periods of anticyclonic circulation in the north Ionian (2006-2009) and limited AW advection to the south-eastern Levantine basin, referring to the study by Artale et al. (2006). The LIW temperature mean trend and standard deviation averaged over the eight subbasins are ~0.002 $\pm$0.232 °C/yr (Table 1), which can be interpreted as a weaker response of the intermediate layers to the warming trend observed at surface.

The sub-basins with the steepest increase are located in the central longitudinal band of the Mediterranean Sea, therefore far from the LIW main sources. The range of temperature and salinity and the respective variability in the Tyrrhenian and Ionian sub-basins are in good agreement with Poulain et al. (2009), where *T* and *S* timeseries from 2001 to 2009 are computed from Argo floats data near 600 m. The ranges and trends for *T* and *S* found in the Ligurian Sea are also confirmed by Margirier et al. (2020), where vertical profiles collected by gliders, Argo floats, CTDs and XBTs in the northwestern Mediterranean Sea over the 2007–2017 period are analyzed.

The LIW depth time series are shown in Fig. 8: significant negative trends (the depth decreases) are found in the Tyrrhenian, Ionian, and Cretan Seas, while in the Catalan and Levantine sub-basins the LIW sinks ($pvalue \leq 0.05$). Non-significant trends are found in the other regions. Abrupt shifts are found in the Adriatic sub-basin from ~200 m to ~500-600 m at different time steps (trend ~2.609$\pm$115.404 m/yr), highlighting a bimodal behavior of the LIW depth and an intense dense water production activity as also shown by Kokkini et al. (2019) and Mihanović et al. (2021). Previous studies attribute dramatic shifts in the Adriatic hydrological properties to the BiOS and the Eastern Mediterranean Transient (e.g., Vilibić et al., 2012). This hypothesis can also be supported by correlations between the BiOS (definition by Vilibić et al., 2020) and the AW/LIW salinity yearly averaged timeseries in the Adriatic Sea, which maximum values are about -0.49/-0.43 at lag 0 /-4 yr (at negative year lag, the BiOS leads; $pvalue \leq 0.05$). Further investigations are left to future studies.

412 The results related to the EMED match those shown in Kassis and Korres (2020), where the
413 timeseries of salinity and temperature averaged between different depths-layers (below 100 m) in
414 similar subbasins are shown (see Fig. 8 in Kassis and Korres 2020). The LIW depth mean trend
415 and standard deviation averaged over the eight subbasins is 1.099 ± 46.458 m/yr (Table 1).
416

417 ## 4 Conclusions

418 We presented an analysis of the main properties and variability of the AW and LIW in the
419 Mediterranean Sea, exploiting the Argo float data that provide an optimal observational dataset
420 to study their thermohaline properties. Indeed, this dataset covers the water column down to
421 ~2000 m and provide data for almost two decades.
422 Taking advantage of different diagnostics discussed in section 2, the AW and LIW have been
423 detected in the Mediterranean Sea through a sub-basin approach, which allowed to define the
424 main hydrological features over this enclosed basin in different regions.
425 In addition to previous studies, this work provides a more detailed view of the AW and LIW
426 characteristics in the last two-decades over most of the Mediterranean Sea, except for the Alboran
427 sub-basin, the Sicily Channel, and the Aegean sub-basin where Argo data are too scarce.
428 To achieve this goal, the first step of this study was the detection of the AW and LIW cores in
429 each available profile. In agreement with previous studies (e.g., Lascaratos et al., 1993;
430 Bergamasco and Malanotte-Rizzoli, 2010; Millot, 2013; Hayes et al., 2019; Várgas-Yañez et al.,
431 2020), we confirmed the mean zonal gradients of the AW and LIW properties over the
432 Mediterranean Sea: the AW becomes saltier, warmer, and deeper moving eastward, while the
433 LIW becomes fresher, colder, and deeper moving westward. These results not only match the
434 present literature but also provide a more detailed view of these water masses over eight sub-
435 basins.
436 The timeseries derived from the AW and LIW parameters have also highlighted some
437 interesting features that are in good agreement with the previous literature. The most relevant
438 results are summarized below:

- Positive salinity and temperature trends characterize the AW and LIW in the last two decades over most of the Mediterranean Sea (average value over the whole region: 0.007 and 0.006 yr^{-1}; 0.026 and 0.022 °C/yr respectively). The warming and salinification of the Mediterranean Sea is in good agreement with previous results (e.g., Skliris et al., 2018; Margirier et al., 2020; Kassis and Korres, 2020).
- Negative AW salinity trends in the Algerian and Catalan sub-basins suggest a freshening of the AW inflow, in agreement with the observed rapid freshening of the North Atlantic Ocean (Dickson et al., 2002).
- Positive AW salinity trends are found east of the Ligurian sub-basin, highlighting a clear salinification of this water mass in the last two decades probably due to the combined effect of the strong increase in net evaporation and the Nile dumming (e.g., Nof, 1979; Skiliris et al., 2018; section 3.2.1a).
- Positive trends in the LIW salinity timeseries are found in the whole Mediterranean Sea at 5% level of significance, highlighting a salinification also at intermediate depths (section 3.2.1b).
- Positive LIW temperature trends ($pvalue \leq 0.05$) are found everywhere except in the Levantine sub-basin, where the negative trend might be related to oscillations with decadal timescales, that play a role in this region. These results highlight a clear warming at intermediate depth in most of the Mediterranean Sea.
- The AW and LIW depth trends are highly space-dependent, showing different behaviors in the eight sub-basins.
- Abrupt shifts in the LIW depth are found in the Adriatic sub-basin from ~200 m to ~500-600 m at different time steps (trend 2.609 ± 115.404 m/yr), highlighting a bimodal behavior of the LIW depth and an intense dense water production activity as also shown by Kokkini et al. (2019) and Mihanović et al. (2021).
- The timeseries length could affect the measure of the trends in the sub-basins that are interested by forcings with periodicity with the same order of magnitude. In this

466 respect, the trends observed in the Adriatic Sea are clearly impacted by the BiOS,
467 since the timeseries starts in 2008, when the anticyclonic BiOS was present. This
468 might be also relevant for other sub-regions.
469 These results therefore provide interesting new insights about the AW and LIW interbasin and
470 interannual variability, that can be further analyzed to investigate which mechanisms lead to the
471 observed temporal trends in each sub-basin.

References

Argo: Argo float data and metadata from Global Data Assembly Centre (Argo GDAC). SEANOE. https://doi.org/10.17882/42182, 2020.

Artale V., Calmante S., Malanotte-Rizzoli P., Pisacane G., Rupolo V., and Tsimplis M., In: Lionello, P., Malanotte-Rizzoli, P., Boscoli, R. (Eds.), The Atlantic and Mediterranean Sea as connected systems, in Mediterranean Climate Variability Dev. Earth Environ. Sci. 4. Elsevier, Amsterdam, pp. 283–323, 2006.

Aulicino G., Cotroneo Y., Ruiz S., Sánchez Román A., Pascual A., Fusco G., Tintoré J. and Budillon G.: Monitoring the Algerian Basin through glider observations, satellite altimetry and numerical simulations along a SARAL/AltiKa track. Journal of Marine Systems, 179(), 55–71.doi:10.1016/j.jmarsys.2017.11.006, 2018

Aulicino G., Cotroneo Y., Olmedo E., Cesarano C., Fusco G., and Budillon G.: In Situ and Satellite Sea Surface Salinity in the Algerian Basin Observed through ABACUS Glider Measurements and BEC SMOS Regional Products. Remote Sensing, 11(11), 1361– .doi:10.3390/rs1111136, 2019.

Azzaro M., La Ferla R., Maimone G., Monticelli L.S., Zaccone R., and Civitarese G.: Prokaryotic dynamics and heterotrophic metabolism in a deep convection site of Eastern Mediterranean Sea (the Southern Adriatic Pit), Continental Shelf Research, Volume 44 2012, Pages 106-118, ISSN 0278-4343, https://doi.org/10.1016/j.csr.2011.07.011, 2012.

Bensi M., Cardin V., Rubino A., Notarstefano G., and Poulain P.M.: Effects of winter convection on the deep layer of the Southern Adriatic Sea in 2012, *J. Geophys. Res. Oceans* 118, 6064– 6075, https://doi.org/10.1002/2013JC009432, 2013.

500

501 Bergamasco A., and Malanotte-Rizzoli P.: The circulation of the Mediterranean Sea: A historical
502 review of experimental investigations. Adv. Oceanogr. Limnol. 2010 1 11–28;
503 https://doi.org/10.1080/19475721.2010.491656, 2010.

504

505 Berkowitz J., and Kilian L.: Recent developments in bootstrapping time series. Econometr Rev
506 19:1–48, https://doi.org/10.1080/07474930008800457, 2000.

507

508 Borghini M., Bryden H., Schroeder K., Sparnocchia S., and Vetrano A.: The Mediterranean is
509 becoming saltier, Ocean Sci. 10, 693–700, https://doi.org/10.5194/os-10-693-2014, 2014.

510

511 Bosse A., Testor P., Mortier L., Prieur L., Taillandier V., d'Ortenzio F., and Coppola L.:
512 Spreading of Levantine Intermediate Waters by submesoscale coherent vortices in the
513 northwestern Mediterranean Sea as observed with gliders. Journal of Geophysical Research.
514 Oceans, Wiley-Blackwell 2015 120 (3), pp.1599-1622,
515 https://doi.org/10.1002/2014JC010263, 2015.

516

517 Bethoux J.P., Gentili B., Raunet J., and Taillez D.: Warming trend in the Western Mediterranean
518 deep water. Nature 347, 660–662, https://doi.org/10.1038/347660a0, 1990.

519

520 Bethoux J. P., Gentili B., Morin P., Nicolas E., Pierre C., and Ruiz-Pino D.: The Mediterranean
521 Sea: A miniature ocean for climatic and environmental studies and a key for the climatic
522 functioning of the North Atlantic, *Prog. Oceanogr.*, **44**, 131– 146, doi:10.1016/S0079-
523 6611(99)00023-3, 1999.

524

525 Cabanes C., Thierry V., and Lagadec C.: Improvement of bias detection in Argo float conductivity
526 sensors and its application in the North Atlantic. Deep Sea Research Part I: Oceanographic
527 Research Papers 114 128-136, https://doi.org/10.1016/j.dsr.2016.05.007, 2016.

Cotroneo Y., Aulicino G., Ruiz S., Pascual A., Budillon G., Fusco G., and Tintoré J.: Glider and satellite high resolution monitoring of a mesoscale eddy in the algerian basin: Effects on the mixed layer depth and biochemistry, Journal of Marine Systems, Volume 162, Pages 73-88, ISSN 0924-7963, https://doi.org/10.1016/j.jmarsys.2015.12.004, 2016.

Cotroneo Y., Aulicino G., Ruiz S., Sánchez Román A., Torner Tomàs M., Pascual A., Fusco G., Heslop E., Tintoré J., and Budillon G.: Glider data collected during the Algerian Basin Circulation Unmanned Survey, Earth Syst. Sci. Data, 11, 147–161, https://doi.org/10.5194/essd-11-147-2019, 2019.

Demirov E. K., and Pinardi N.: On the relationship between the water mass pathways and eddy variability in the Western Mediterranean Sea, *J. Geophys. Res.* 112, C02024, https://doi.org/10.1029/2005JC003174, 2007.

Dickson B., Yashayaev I., Meincke J., Turrell B., Dye S., and Holfort J.: Rapid freshening of the deep North Atlantic Ocean over the past four decades. *Nature* **416,** 832–837, https://doi.org/10.1038/416832a, 2002.

Dukhovskoy D.S., Yashayaev I., Proshutinsky A., Bamber J. L., Bashmachnikov I. L., Chassignet E. P., Lee C.M., and Tedstone A.J.: Role of Greenland freshwater anomaly in the recent freshening of the subpolar North Atlantic. *Journal of Geophysical Research: Oceans*, 124, 3333– 3360. https://doi.org/10.1029/2018JC014686, 2019.

Escudier R., Mourre B., Juza M., and Tintoré J.: Subsurface circulation and mesoscale variability in the Algerian subbasin from altimeter-derived eddy trajectories, J. Geophys.Res. Oceans 121, 6310–6322, https://doi.org/10.1002/2016JC011760, 2016.

556 Font J., Millot C., Pérez JDJS, Julià A., and Chic O.: The drift of Modified Atlantic Water from
557 the Alboran Sea to the eastern Mediterranean. Scientia Marina. 62. 211-216,
558 https://doi.org/10.3989/scimar.1998.62n3211, 1998.
559
560 Giorgi F.: Climate change hot-spots. Geophysical Research Letters, 33: L08707,
561 https://doi.org/10.1029/2006GL025734, 2006.
562
563 Hayes D. R., Schroeder K., Poulain P.M., Testor P., Mortier L., Bosse, A., Du Madron X.: Review
564 of the Circulation and Characteristics of Intermediate Water Masses of the
565 Mediterranean: Implications for Cold-Water Coral Habitats. In: Orejas C., Jiménez C.
566 (eds) Mediterranean Cold-Water Corals: Past, Present and Future. Coral Reefs of the
567 World, vol 9. Springer, Cham, https://doi.org/10.1007/978-3-319-91608-8_18, 2019.
568
569 Hernández-Molina F., Stow D., Zarikian C., Acton G., Bahr A., Balestra B., Ducassou E., Flood
570 R., Flores J.A., Furota S., Grunert P., Hodell D., Jiménez-Espejo F., Kim J.K., Krissek L.,
571 Kuroda J., Li B., Llave E., Lofi J., and Xuan C.: Onset of Mediterranean outflow into the North
572 Atlantic. Science. 344, https://doi.org/10.1126/science.1251306, 2014.
573
574 Juza M., Escudier R., Vargas-Yáñez M., Mourre B., Heslop E., Allen J., and Tintoré J.: Charac-
575 terization of changes in Western Intermediate water properties enabled by an innovative ge-
576 ometry-based detection approach. Journal of Marine Systems 191, 1–12. doi:
577 10.1016/j.jmarsys.2018.11.003, 2019.
578
579 Kassis D., and Korres G.: Hydrography of the Eastern Mediterranean basin derived from argo
580 floats profile data, Deep Sea Research Part II: Topical Studies in Oceanography, Volume
581 171,2020,104712,ISSN 0967-0645, https://doi.org/10.1016/j.dsr2.2019.104712, 2020.
582

583 Kokkini Z., Mauri M., Gerin R., Poulain P.M., Simoncelli S., and Notarstefano G.: On the salinity
584 structure in the South Adriatic as derived from float and glider observations in 2013–2016,
585 Deep Sea Research Part II: Topical Studies in Oceanography,Volume 171 2020 104625, ISSN
586 0967-0645, https://doi.org/10.1016/j.dsr2.2019.07.013, 2019.
587
588 Kreyszig E.: Introductory Mathematical Statistics: Principles and Methods. New York: Wiley,
589 1970.
590
591 Kubin E., Poulain P.M, Mauri E., Menna M., and Notarstefano G.: Levantine Intermediate and
592 Levantine Deep Water Formation: An Argo Float Study from 2001 to 2017,
593 https://doi.org/10.3390/w11091781, 2019.
594
595 Lamer P.A., Mauri E., Notarstefano G., and Poulain P.M.: The Levantine Intermediate Water in
596 the eastern Mediterranean Sea; http://maos.inogs.it/pub/REPORT_LAMER_final_last.pdf,
597 2019.
598
599 Lascaratos A., Williams R.G., and Tragou E.: A mixed-layer study of the formation of Levantine
600 intermediate water. Journal of Geophysical Research 98, https://doi.org/10.1029/93JC00912,
601 1993.
602
603 Lipizer M., Partescano E., Rabitti A., Giorgetti A., and Crise A.: Qualified temperature, salinity
604 and dissolved oxygen climatologies in a changing Adriatic Sea, Ocean Sci., 10, 771–797,
605 https://doi.org/10.5194/os-10-771-2014, 2014.
606
607 Malanotte-Rizzoli P., Manca B., Marullo S., Ribera d'Alcala M., Roether W., Theocharis A.,
608 Bergamasco A., Budillon G., Sansone E., Civitarese G., Conversano F., Gertman I., Hernt B,
609 Kress N., Kioroglou S., Kontoyiannis H., Nittis K., Klein B., Lascaratos A., and Kovacevic
610 V.: The Levantine Intermediate Water Experiment (LIWEX) Group: Levantine basin—A

611 laboratory for multiple water mass formation processes. Journal of Geophysical Research. 108.
612 8101, https://doi.org/10.1029/2002JC001643, 2003.
613
614 Margirier F., Testor P., Heslop E., Mallil K., Bosse A., Houpert L., Mortier L., Bouin M.-
615 N., Coppola L., D'Ortenzio F., de Madron X.D., Mourre B., Prieur L., Raimbault P., and
616 Taillandier V.: Abrupt warming and salinification of intermediate waters interplays with
617 decline of deep convection in the Northwestern Mediterranean Sea. Sci Rep 10 20923,
618 https://doi.org/10.1038/s41598-020-77859-5, 2020.
619
620 Mauri E., Sitz L., Gerin R., Poulain P.M., Hayes D., and Gildor H.: On the Variability of the
621 Circulation and Water Mass Properties in the Eastern Levantine Sea between September 2016–
622 August 2017. *Water* **2019**, *11*, 1741, https://doi.org/10.3390/w11091741, 2019.
623
624 Mauri E., Menna M., Garić R., Batistić M., Libralato S., Notarstefano G., Martellucci R., Gerin
625 R., Pirro A., Hure M., Poulain P-M, 2021. Recent changes of the salinity distribution and
626 zooplankton community in the South Adriatic Pit, accepted in OSR5.
627
628 Mihanović, H., Vilibić, I., Šepić, J., Matić, F., Ljubešić, Z., Mauri, E., Gerin, R., Notarstefano,
629 and G., Poulain, P.-M: Observation, preconditioning and recurrence of exceptionally high
630 salinities in the Adriatic Sea. Frontiers in Marine Scences, 8, 672210. doi:
631 10.3389/fmars.2021.672210, 2021.
632
633 Millot C., and Taupier-Letage I.: Circulation in the Mediterranean Sea: Updated description and
634 schemas of the circulation of the water masses in the whole Mediterranean Sea. A. Saliot. The

635 Mediterranean Sea, The Mediterranean Sea (5-K), Springer, pp.29-66 2005, Handbook of
636 Environmental Chemistry, 9783540314929 9783540250180.ff10.1007/b107143ff. ffhal-
637 01191856v1f, https://doi.org/10.1007/b107143, 2005.

638

639 Millot C., Candela J., Fuda J.L., and Tber Y.: Large warming and salinification of the
640 Mediterranean outflow due to changes in its composition. Deep-Sea Res. 53, 656–665,
641 https://doi.org/10.1016/j.dsr.2005.12.017, 2006.

642

643 Millot C.: Interannual salinification of the Mediterranean inflow, Geophys. Res. Lett., 34,
644 L21609, doi:10.1029/2007GL031179, 2007.

645

646 Millot C.: Levantine Intermediate Water characteristics: An astounding general
647 misunderstanding. Scientia Marina. 78, https://doi.org/10.3989/scimar.04045.30H, 2013.

648

649 Millot C.: Levantine intermediate water characteristics: an astounding general misunderstanding!
650 (addendum). Sci. Marina, 78 165-171, https://doi.org/10.3989/scimar.04045.30H, 2014.

651

652 Nof D.: On man-induced variations in the circulation of the Mediterranean Sea. Tellus 31, 558–
653 564, 1979.

654

Notarstefano G., and Poulain P. M.: Delayed mode quality control of Argo floats salinity data in the Tyrrhenian Sea. Technical Report OGS 2008/125 OGA 43 SIRE, http://nettuno.ogs.trieste.it/sire/DMQC/dmqc_1900593_54073_V1.pdf, 2008.

Notarstefano G., and Poulain P. M.: Thermohaline variability in the Mediterranean and Black Seas as observed by Argo floats in 2000-2009. OGS Tech. Rep. OGS 2009/121 OGA 26 SIRE, 72 pp.-171, http://dx.doi.org/10.3989/scimar.04045.30H, 2009.

Notarstefano G., and Poulain P.M.: Delayed mode quality control of Argo salinity data in the Mediterranean Sea: A regional approach. Technical Report OGS 2013/103 Sez. OCE 40 MAOS, 2013.

Ozer T., Gertman I., Kress N., Silverman J., and Herut B.: Interannual thermohaline (1979–2014) and nutrient (2002–2014) dynamics in the Levantine surface and intermediate water masses, SE Mediterranean Sea. Global and Planetary Change, 151, 60–67. doi:10.1016/j.gloplacha.2016.04.001, 2017.

Painter S.C., and Tsimplis M.N.: Temperature and salinity trends in the upper waters of the Mediterranean Sea as determined from the MEDATLAS dataset, Continental Shelf Research, Volume 23, Issue 16 2003, Pages 1507-1522, ISSN 0278-4343, https://doi.org/10.1016/j.csr.2003.08.008, 2003.

677 Poulain P.M., Barbanti R., Font J., Cruzado A., Millot C., Gertman I., Griffa A., Molcard A.,
678 Rupolo V., Le Bras S., and Petit de la Villeon L.: MedArgo: a drifting profiler program in the
679 Mediterranean Sea. Ocean Science, European Geosciences Union 2007, 3 (3), pp.379- 395.
680 hal-00331145, https://doi.org/10.5194/osd-3-1901-2006, 2007.
681
682 Poulain P.M., Solari M., Notarstefano G., and Rupolo V.: Assessment of the Argo sampling in
683 the Mediterranean and Black Seas (part II).
684 http://maos.inogs.it/pub/2009_report_task4.4_partII.pdf, 2009.
685
686 Rahmstorf S.: Influence of Mediterranean Outflow on climate, *Eos Trans. AGU*, **79**, 281– 282,
687 doi:10.1029/98EO00208, 1998.
688
689 Rahmstorf, S.: Thermohaline Ocean Circulation. In: Encyclopedia of Quaternary Sciences, Edited
690 by S. A. Elias. Elsevier, Amsterdam, http://www.pik-
691 potsdam.de/~stefan/Publications/Book_chapters/rahmstorf_eqs_2006.pdf, 2006.
692
693 Roemmich D., Johnson G., Riser S., Davis R., Gilson J., Owens W., Garzoli S., Schmid C., and
694 Mark I.: The Argo Program Observing the Global Ocean with Profiling Floats. Oceanography.
695 22, https://doi.org/10.5670/oceanog.2009.36, 2009.
696
697 Rohling E.J., and Bryden H.L.: Man induced salinity and temperature increase in the Western
698 Mediterranean Deep Water. J. Geophys. Res. 97 (C7) 11191–11198,
699 https://doi.org/10.1029/92JC00767, 1992.
700
701 Rubino A., Gačić M., Bensi M., Vedrana K., Vlado M., Milena M., Negretti M.E., Sommeria J.,
702 Zanchettin D., Barreto R.V., Ursella L., Cardin V., Civitarese G., Orlić M., Petelin B., and

Siena G.: Experimental evidence of long-term oceanic circulation reversals without wind influence in the North Ionian Sea. *Sci Rep* **10** **1**905 (2020), https://doi.org/10.1038/s41598-020-57862-6, 2020.

Schroeder K., Chiggiato J., Josey S., Borghini M., Aracri S., and Sparnocchia S.: Rapid response to climate change in a marginal sea. Scientific Reports. 7, https://doi.org/10.1038/s41598-017-04455-5, 2017.

Schroeder K.,: Current Systems in the Mediterranean Sea, Editor(s): J. Kirk Cochran, Henry J. Bokuniewicz, Patricia L. Yager, Encyclopedia of Ocean Sciences (Third Edition), Academic Press 2019, Pages 219-227, ISBN 9780128130827, https://doi.org/10.1016/B978-0-12-409548-9.11296-5, 2019.

Schuckmann K.V., Traon P.-Y.L., Smith N., Pascual A., Djavidnia S., Gattuso J.-P., Grégoire M., Nolan G., Aaboe S., Aguiar E., et al.: Copernicus marine service ocean state report, issue 3. *J. Oper. Oceanogr, 12*, S1–S123, 2019.

Shaltout M., and Omstedt A.: Recent sea surface temperature trends and future scenarios for the Mediterranean Sea, Oceanologia, Volume 56, Issue 3 2014, Pages 411-443, ISSN 0078-3234, https://doi.org/10.5697/oc.56-3.411, 2014.

Skliris N.: Past, Present and Future Patterns of the Thermohaline Circulation and Characteristic Water Masses of the Mediterranean Sea. In: Goffredo S., Dubinsky Z. (eds) The Mediterranean Sea. Springer, Dordrecht, https://doi.org/10.1007/978-94-007-6704-1_3, 2014.

Skliris N., Zika J.D., Herold L., Josey S.A., and Marsh R.: Mediterranean sea water budget long-term trend inferred from salinity observations. *Clim Dyn* **51** **2**857–2876 (2018). https://doi.org/10.1007/s00382-017-4053-7, 2018.

731

732 Tsimplis M., Zervakis V., Josey S.A., Peneva E., Struglia M.V., Stanev E., Lionello P.,
733 Malanotte-Rizzoli P., Artale V., Theocharis A., Tragou E., and Oguz T.: Changes in the
734 oceanography of the Mediterranean Sea and their link to climate variability. In: Lionello, P.;
735 Malanotte-Rizzoli, P.; and Boscolo, R., (eds.) Mediterranean climate variability. Amsterdam,
736 The Netherlands, Elsevier 227-282, 438pp. (Developments in Earth and Environmental
737 Sciences, 4), https://doi.org/10.1016/S1571-9197(06)80007-8, 2006.

738

739 Vàrgas-Yáñez M., Moya F., Tel E., García-Martínez M.C., Guerber E., and Bourgeon M.:
740 Warming and salting of the Western Mediterranean during the second half of the XX century:
741 inconsistencies, unknowns and the effect of data processing. Sci. Mar. 73 (1), 7–28,
742 https://doi.org/10.3989/scimar.2009.73n1007, 2009.

743

744 Vàrgas-Yáñez M., Moya F., García-Martínez M.C., Tel E., Zunino P., Plaza F., Salat J., Pascual
745 J., López-Jurado J.L., and Serra M.: Climate change in the Western Mediterranean Sea 1900–
746 2008, Journal of Marine Systems, Volume 82, Issue 3 2010, Pages 171-176, ISSN 0924-7963,
747 https://doi.org/10.1016/j.jmarsys.2010.04.013, 2010.

748

749 Vàrgas-Yáñez M., Juza M., Balbín R., Velez-Belchí P., García-Martínez M. C., Moya F., and
750 Hernández-Guerra A.: Climatological Hydrographic Properties and Water Mass Transports in
751 the Balearic Channels From Repeated Observations Over 1996–2019, Frontiers in Marine
752 Science, Volume 7, Pages 779, IISN 2296-7745,
753 https://www.frontiersin.org/article/10.3389/fmars.2020.568602, 2020.

754

755 Vilibić, I., Matijević, S., Šepić, J., and Kušpilić G.: Changes in the Adriatic oceanographic
756 properties induced by the Eastern Mediterranean Transient, Biogeosciences, 9, 2085–2097,
757 https://doi.org/10.5194/bg-9-2085-2012, 2012.

758 Vilibić, I., Šepić, J., and Proust, N.: Weakening of thermohaline circulation in the Adriatic Sea.
759 Climate Research, 55, 217–225, 2013.
760
761 Vilibić, I., Zemunik, P., Dunić, N., and Mihanović, H.: Local and remote drivers of the observed
762 thermohaline variability on the northern Adriatic shelf (Mediterranean Sea). Cont. Shelf Res.
763 199:104110. doi: 10.1016/j.csr.2020.104110, 2020.
764
765 Wong A., Keeley R., Carval T., Argo Data Management Team: Argo Quality Control Manual for
766 CTD and Trajectory Data, https://doi.org/10.13155/33951, 2021.
767
768 Zu Z., Poulain P.M., and Notarstefano G.: Changes in hydrological properties of the
769 Mediterranean Sea over the last 40 years with focus on the Levantine Intermediate Water and
770 the Atlantic Water**,** http://maos.inogs.it/pub/Hydro_trend_LIW_SAW_core_report_v10.pdf,
771 2014.
772

773

774

Table 1. Trends by year for the AW and LIW salinity, temperature, and depth timeseries in eight Mediterranean subbasins. In bold characters the trends significant at 5% level. The rightmost column shows the mean and standard deviation trend values computed over the eight subbasins (here identified with MED). Trends are defined as mean ± standard deviation.

	Algerian	Catalan	Ligurian	Tyrrhenian	Adriatic	Ionian	Cretan	Levantine	MED
Salinity [1/yr]									
AW	**-0.014±0.151**	**-0.004±0.088**	-0.001±0.089	**0.006±0.157**	**0.044±0.188**	**0.009±0.181**	**0.013±0.166**	**0.003±0.100**	**0.007±0.140**
LIW	**0.002±0.022**	**0.002±0.017**	**0.005±0.034**	**0.006±0.035**	**0.021±0.074**	**0.004±0.031**	**0.005±0.048**	**0.004±0.039**	**0.006±0.038**
Temperature [°C/yr]									
AW	**0.054±0.614**	0.019±0.846	0.004±0.914	**0.042±0.528**	**0.117±0.951**	**0.023±0.395**	**-0.026±0.786**	**0.026±0.683**	**0.026±0.715**
LIW	**0.008±0.125**	**0.010±0.088**	**0.022±0.138**	**0.030±0.167**	**0.093±0.384**	**0.030±0.226**	-0.003±0.226	**0.012±0.391**	**0.022±0.232**
Depth [m/yr]									
AW	**-0.092±2.271**	-0.019±4.646	-0.012±5.720	**0.394±4.002**	0.757±25.800	**-0.324±7.352**	0.116±17.480	**1.087±17.024**	**0.238±10.537**
LIW	-0.352±14.639	**1.895±52.582**	-0.155±40.249	**-7.034±46.395**	2.609±115.404	**-4.973±42.536**	**-1.630±26.943**	**0.849±32.912**	**1.099±46.458**

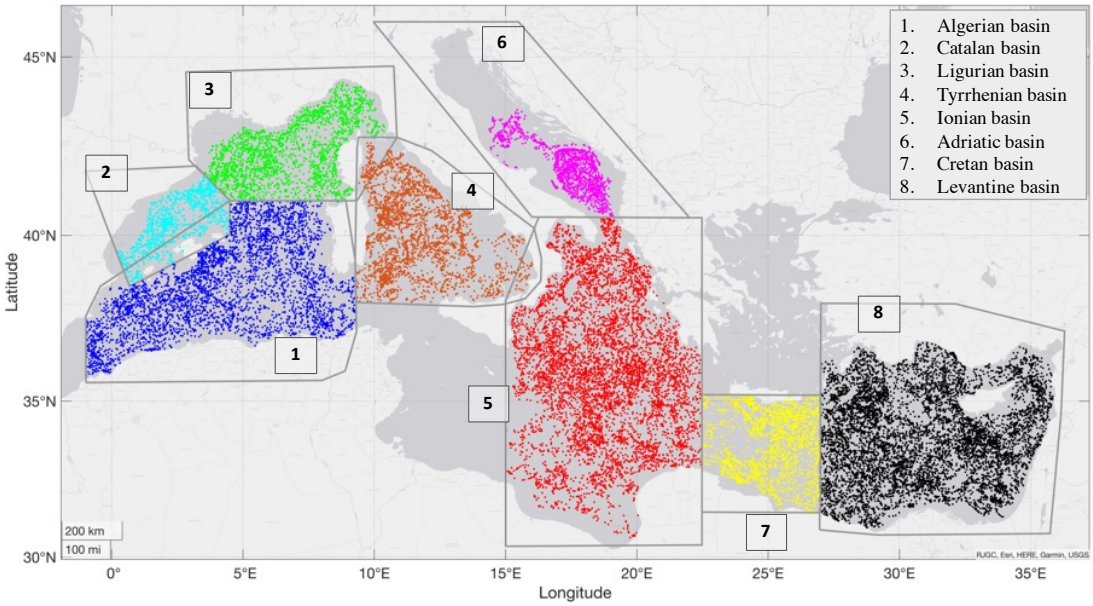

775

776 Fig. 1 Argo floats profiles scatter plot in the Mediterranean Sea between 2001 and 2019 in eight

777 regions based on the climatological areas defined by the EU/MEDARMEDATLAS II project.

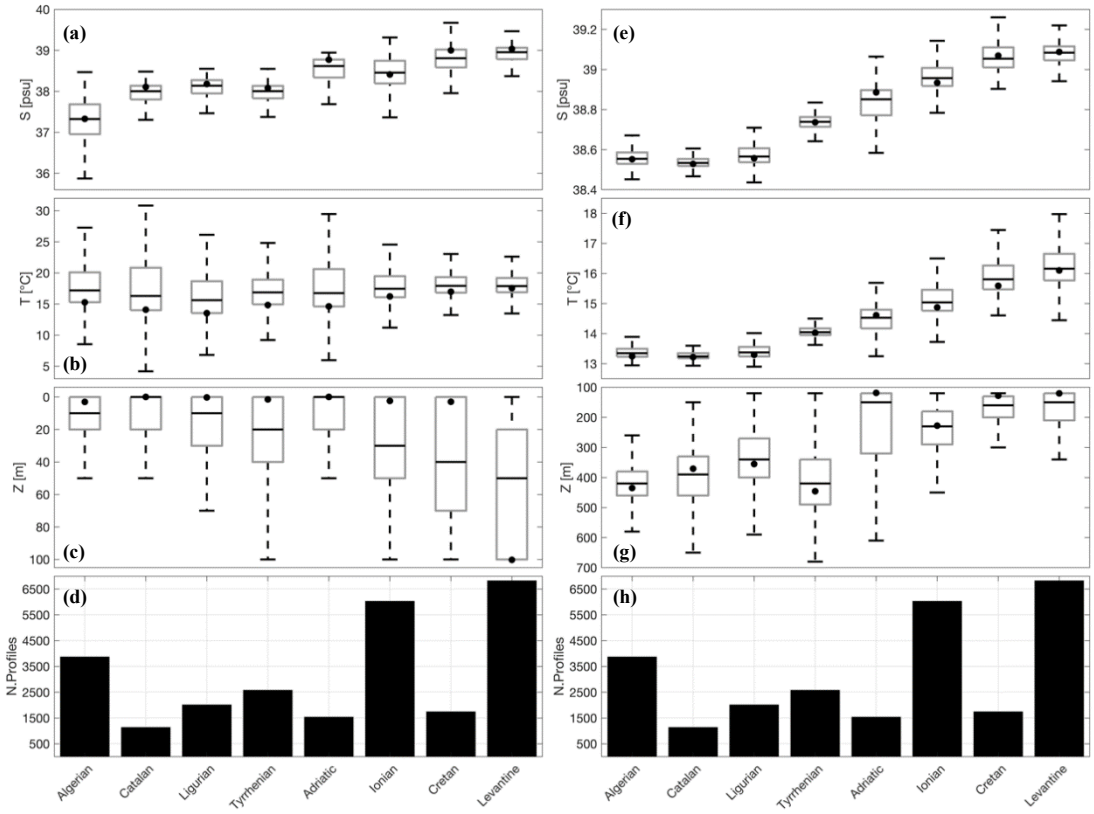

778

779 Fig. 2 Boxplot diagrams for the AW salinity (a), temperature (b) and depth (c) in eight
780 Mediterranean subbasins. Inside each grey box, the black bold line indicates the median, while
781 the bottom and top edges of the box indicate the 25th and 75th percentiles respectively, and the
782 black dots show the mode of each distribution, which corresponds to the maximum PDF. The
783 number of profiles (black bars) for each subbasin are shown in panel (d). The corresponding
784 diagrams for the LIW are shown in the panels (e,f,g,h).

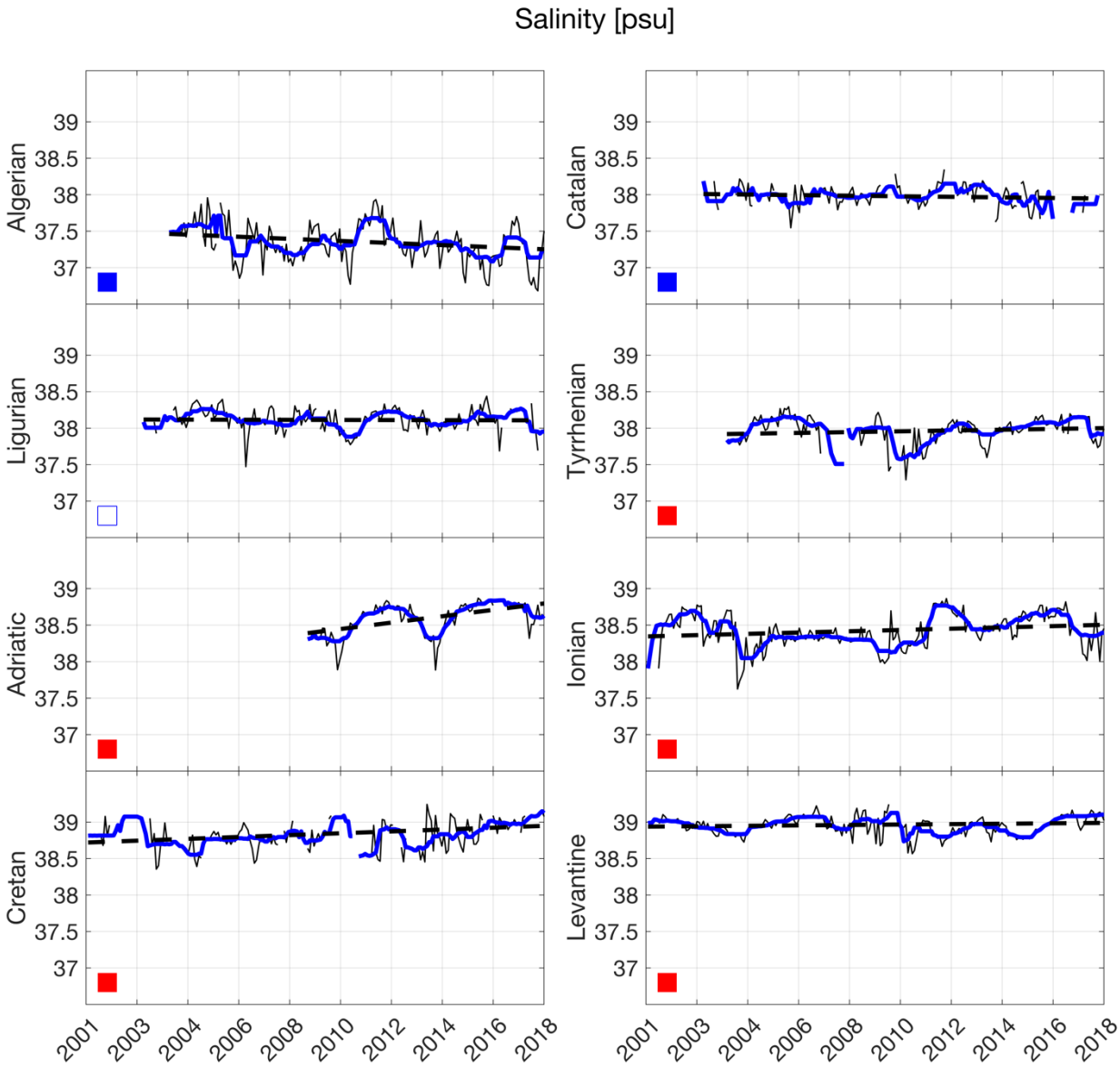

785

786 Fig. 3 AW salinity timeseries in eight subbasins: the thin black lines show the monthly timeseries
787 (seasonal cycle filtered out), the tick blue lines are the 1-year moving average timeseries and the
788 dashed black lines are the trends. The red/blue filled squares identify the positive/negative trends
789 with pvalue≤0.05, while the red/blue not-filled squares identify the positive/negative trends with
790 pvalue>0.05.

791

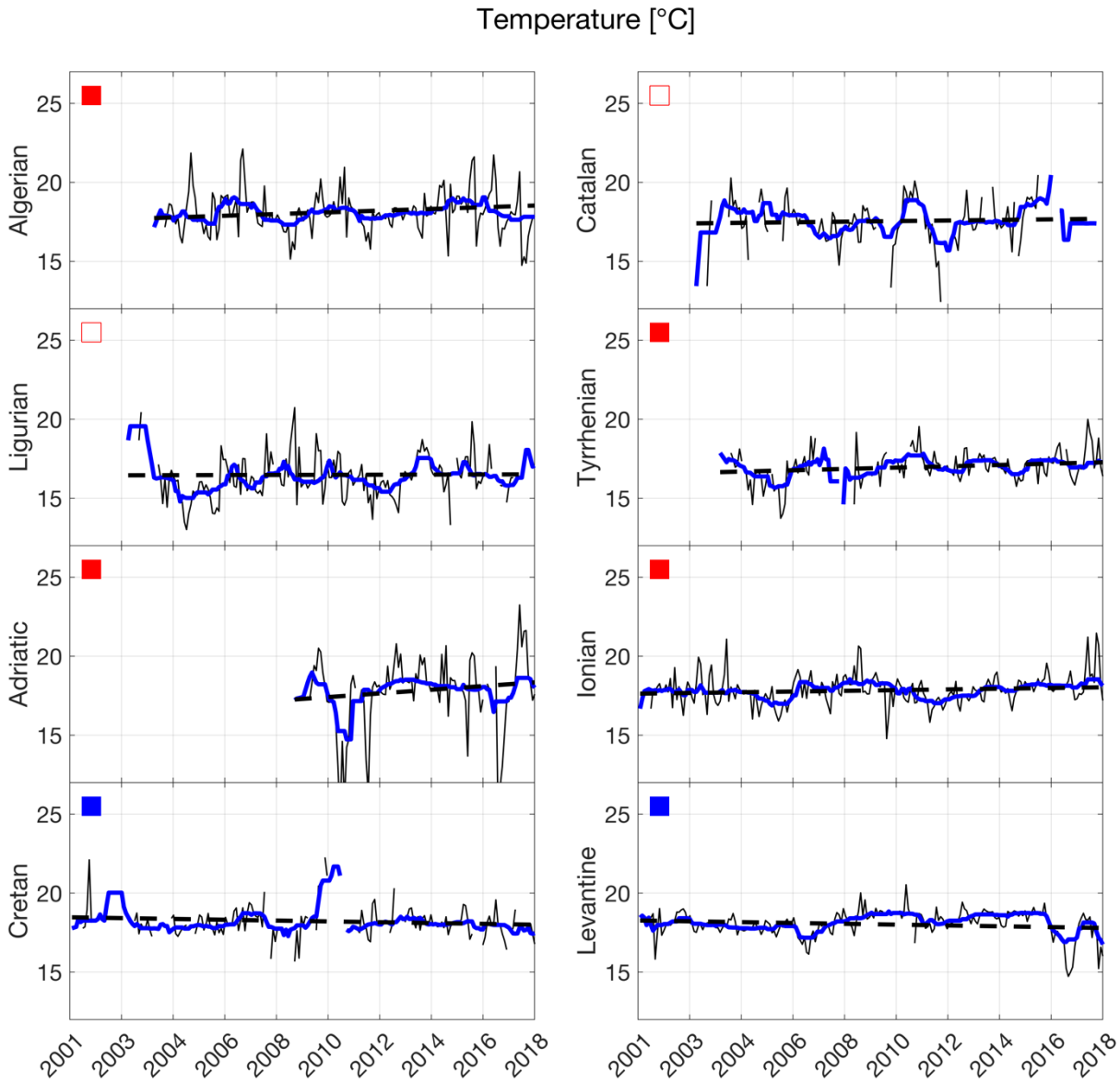

792

793 Fig. 4 Same as Fig. 3 but for the AW temperature.

794

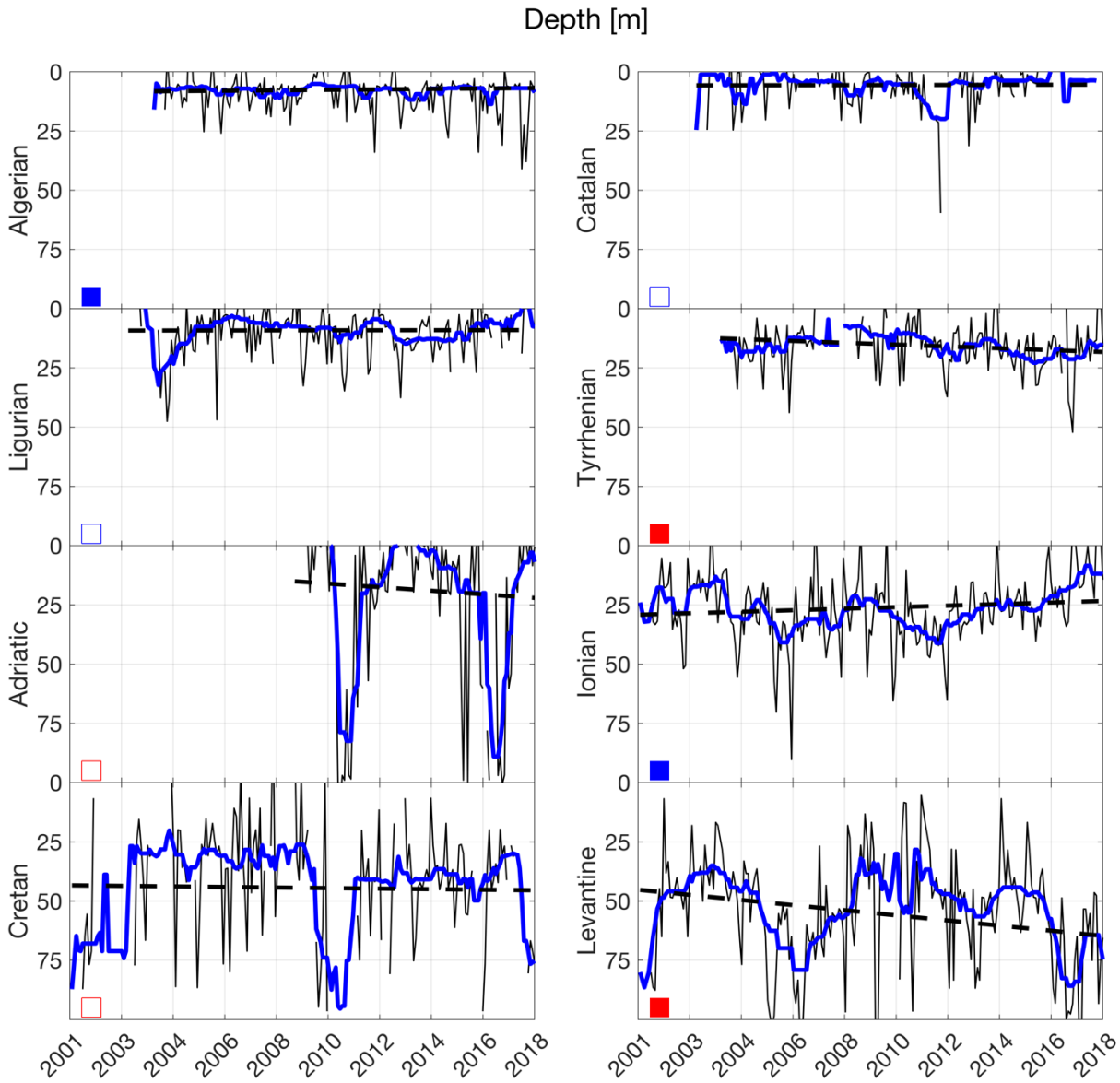

795

796 Fig. 5 Same as Fig. 3 but for the AW depth. Positive/negative trends (red/blue squares) in this

797 case corresponds to an increase/decrease of the depth (i.e., deeper/shallower).

798

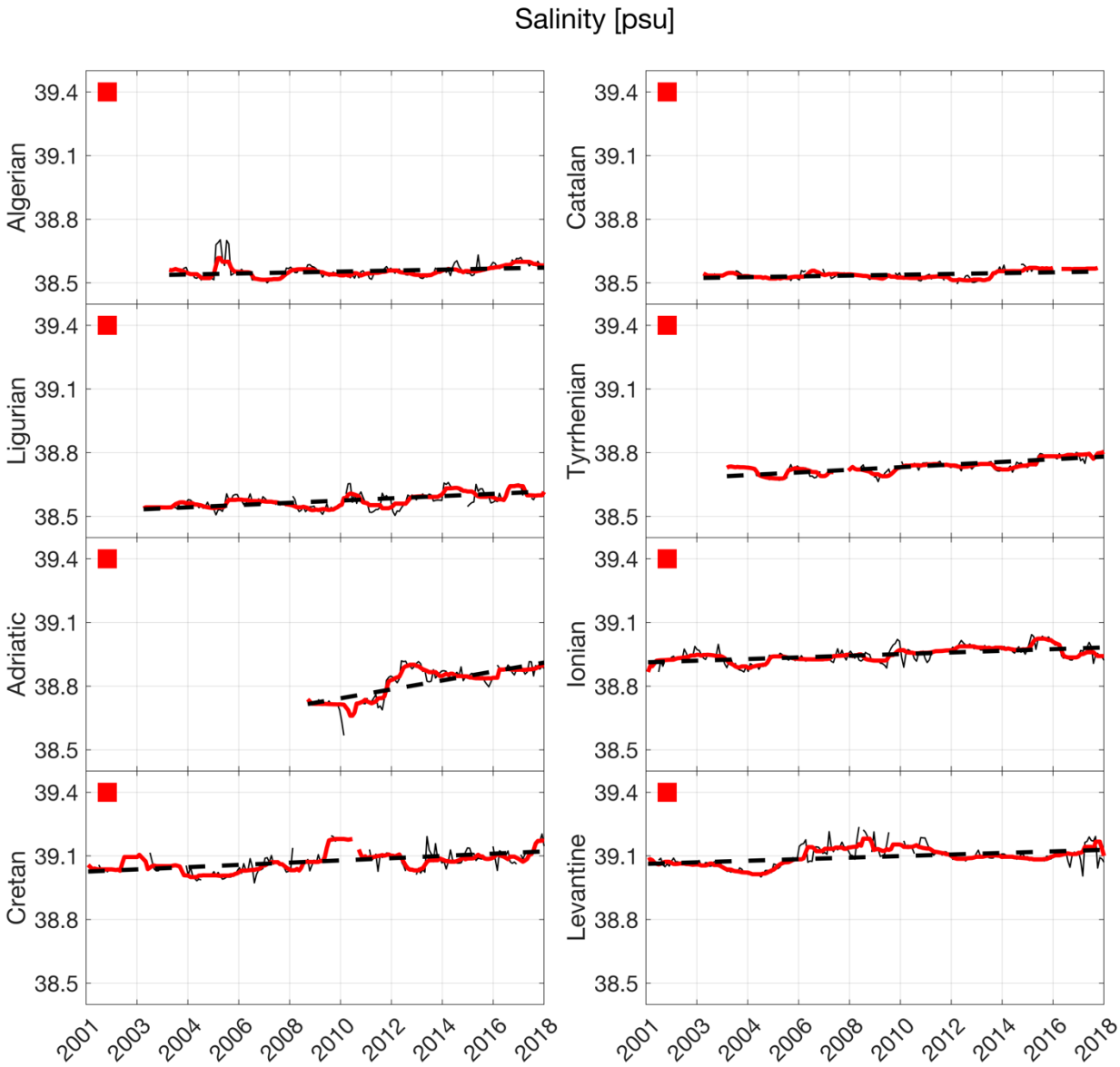

799

800 Fig. 6 Same as Fig. 3 but for the LIW salinity.

801

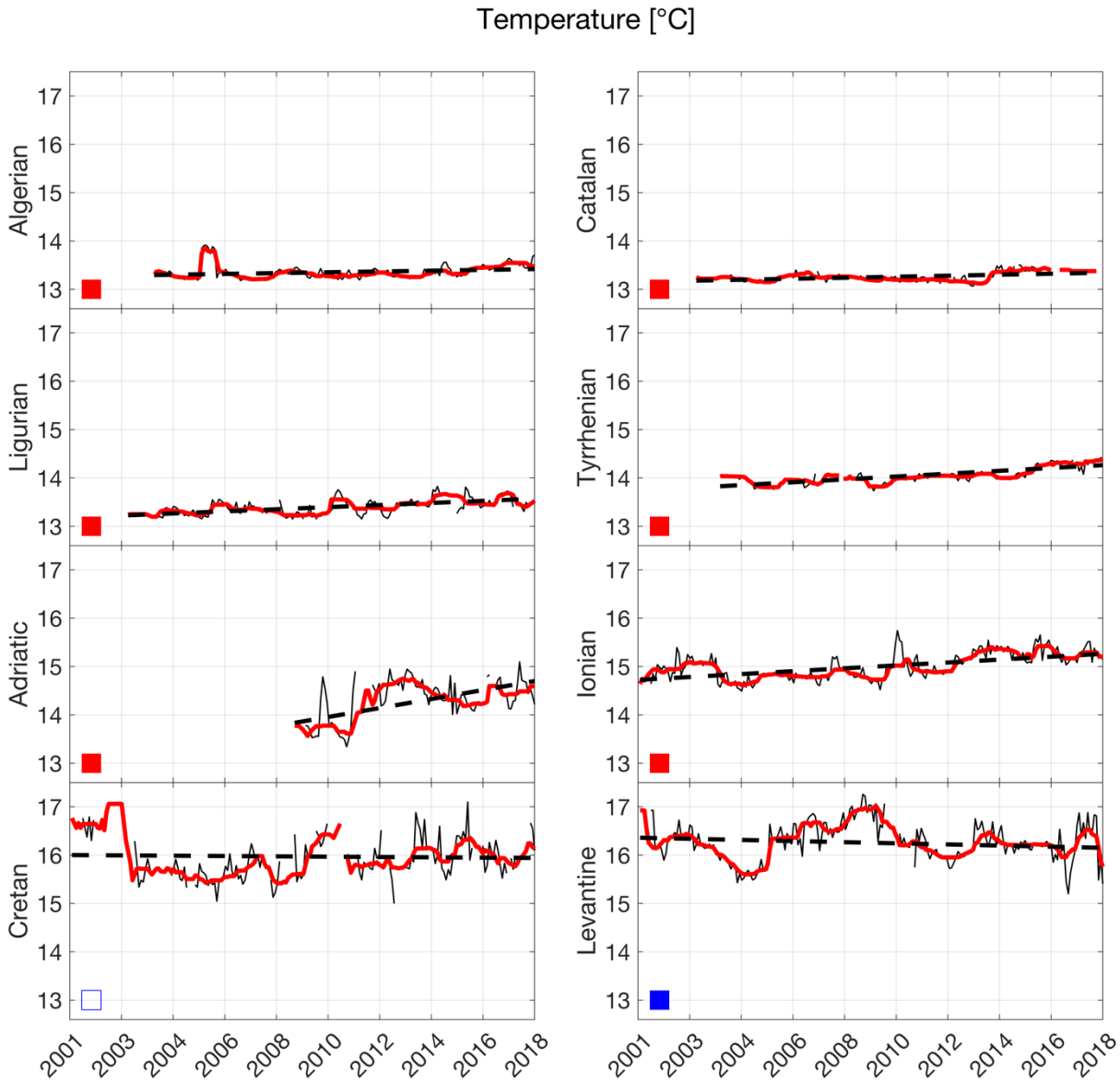

802

803 Fig. 7 Same as Fig. 3 but for the LIW temperature.

804

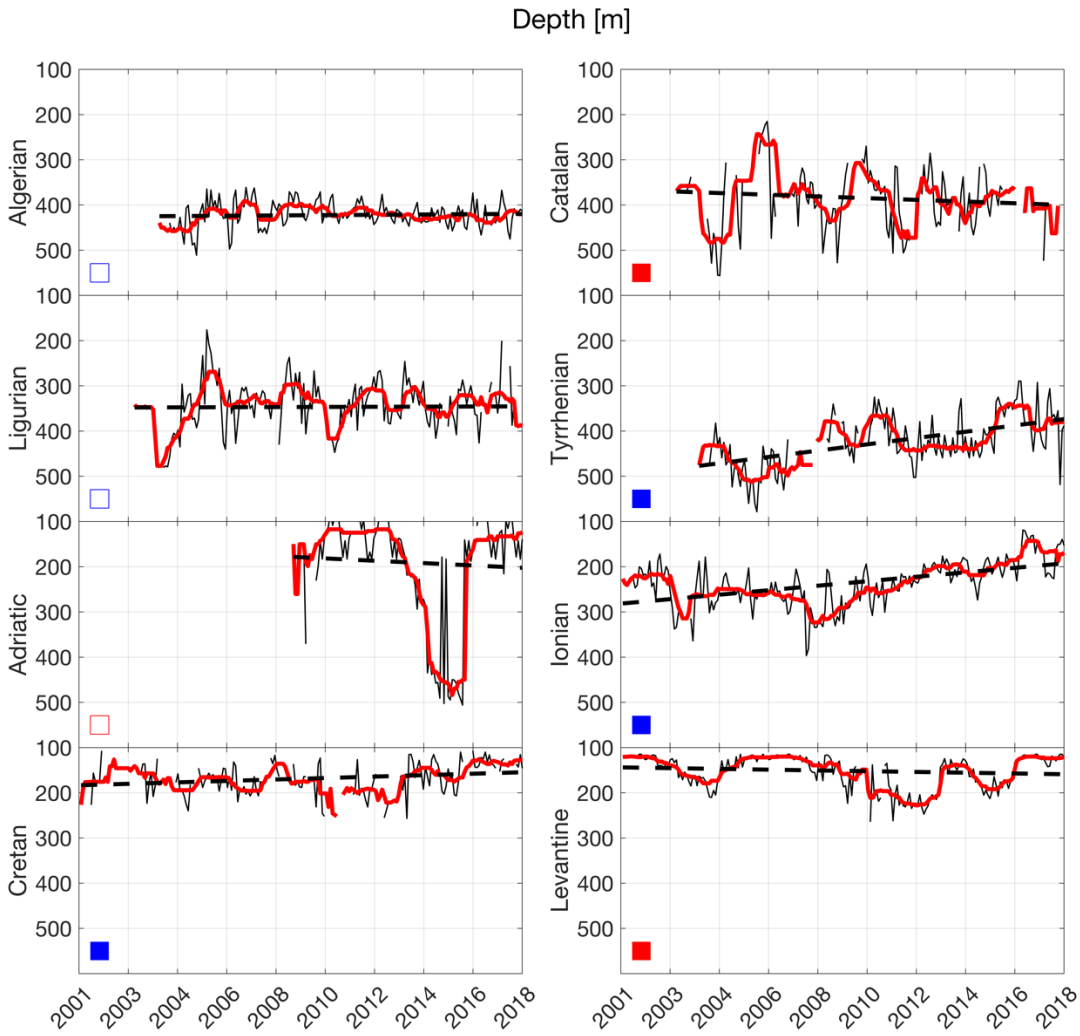

805

806 Fig. 8 Same as Fig. 3 but for the LIW depth. Positive/negative trends (red/blue squares) in this

807 case corresponds to an increase/decrease of the depth (i.e., deeper/shallower).